Int J Adv Manuf Technol (2004) 24: 632–639
DOI 10.1007/s00170-003-1744-5

ORIGINAL ARTICLE

Yong Huang · Steven Y. Liang

Modelling of CBN tool crater wear in finish hard turning

Received: 04 December 2002 / Accepted: 04 March 2003 / Published online: 16 June 2004

Abstract The wear of cubic boron nitride (CBN) cutters, commonly used now in the finish turning of hardened parts, is an important issue that needs to be addressed for hard turning to be a viable technology due to the high costs of CBN cutters and the down-time for tool change. Chipping and tool breakage, which lead to early tool failure, are both prone to take place under the effect of crater wear. The objective of this study is to develop a methodology to model the CBN tool crater wear rate to both guide the design of CBN tool geometry and optimise cutting parameters in finish hard turning. First, the wear volume losses due to the main wear mechanisms (abrasion, adhesion, and diffusion) are modelled as functions of cutting temperature, stress, and other process attributes respectively. Then, the crater wear rate is predicted in terms of tool/work material properties and cutting configuration. Finally, the proposed model is experimentally validated in finish turning of hardened 52100 bearing steel using a low CBN content insert. The comparison between the prediction and the measurement shows reasonable agreement and the results suggest that adhesion is the main wear mechanism over the investigated range of cutting conditions.

Keywords Cubic boron nitride · Hard turning · Crater wear · Wear rate

Nomenclature

a	Hardness constant ($1/°C$)
C_0	Concentration of the diffusing species
d	Depth of cut (m)
D_0	Diffusion coefficient related to the frequency of atomic oscillations (m^2/s)
D	Coefficient of diffusion (m^2/s)
f	Feed (m)
h	Contact length (m)
K	Dimensionless constant
K_{abrasion}	Process related dimensionless abrasive wear coefficient
K_{adhesion}	Process related adhesive wear coefficient (m^3/N)
K_{diff}	Process related diffusive wear coefficient ($ms^{-\frac{1}{2}}$)
K_Q	Constant related with activation energy for diffusion (K)
l_1	Length within where normal stress in uniform (m)
l_f	Sliding length (m)
l_s	Sticking length (m)
n	Dimensionless constant
P_a	Hardness of the abrasive particle (N/mm^2)
P_t	Tool hardness (N/mm^2)
Q	Activation energy for diffusion (Cal/mole)
r	Tool nose radius (m)
R	Gas constant ($\text{Cal/mole} \cdot \text{K}$)
$t_{\max}$	Maximum undeformed chip thickness along the tool cutting edge (m)
$T(x)$	Temperature distribution along the interface °C
$V_{\text{chip}}(x)$	Chip velocity along the tool rake face (m/s)
$\hat{V}_{\text{wear-abrasion}}$	Tool volume loss due to abrasion within time interval (m^3)
$\hat{V}_{\text{wear-adhesion}}$	Tool volume loss due to adhesion within time interval (m^3)
$\hat{V}_{\text{wear-diff}}$	Tool volume loss due to diffusion within time interval (m^3)
w	Width of cut (m)
$\Delta K_T(x)$	Crater wear depth change along the contact length (μm)
Δt	Time interval (s)
ΔV_{wear}	Tool material removed within time interval $\Delta t (m^3)$
Δx	Length of an infinitesimal segment AB along the interface (m)
$\sigma(x)$	Normal stress along the tool-chip interface (N/m^2)

Y. Huang
Department of Mechanical Engineering,
Clemson University,
Clemson, SC 29634-0921, USA

S.Y. Liang (✉)
George W. Woodruff School of Mechanical Engineering,
Georgia Institute of Technology,
Atlanta, GA 30332-0405, USA
E-mail: steven.liang@me.gatch.edu

1 Introduction

A hard turning process is a single point turning of materials harder than 50 HRc. It differs from conventional turning in the hardness of work materials and the cutting tool required. As a potential alternative machining process, hard turning offers many benefits over form grinding, including lower equipment costs, shorter setup time, reduced process steps, high material removal rate, better surface integrity, and elimination of cutting fluid [1–3]. However, the severe tool wear often presents difficulties for hard turning implementation. The high cost of hard turning cutters and the tool change downtime can impact the economic viability of precision hard turning. The recent development of tool materials and geometries for hard turning applications has always been characterised by an increase in wear resistance. The ability to predict tool wear rate for various tool materials and tool geometries under various cutting conditions is important to the overall optimisation of finish hard turning process.

Different classifications of tool wear processes in metal cutting have been found in the literature. Basically, six wear mechanisms or any combinations of them are involved in the wear process of cutting tools. They are: abrasion, adhesion, attrition, fatigue, dissolution/diffusion, and tribochemical processes [4, 5]. In hard turning, not only tool geometry and cutting condition, but also the cubic boron nitride (CBN) content, binder phase, chemical stability of a CBN tool, and composition of the workpiece materials are factors influencing tool wear mechanisms [6]. Of the currently available cutting tool materials, CBN is the best candidate and is well used for hard turning process now. As generally accepted, different wear processes coexist during hard turning using CBN tool, and some may dominate over others depending upon the cutting configuration and condition. Most prominent modes of tool wear in hard turning, however, have been found to be abrasion, adhesion, and diffusion mechanisms [7] given the commonly applied cutting conditions, tool geometry, and material properties of the CBN tool and the workpiece in hard turning.

CBN tool flank wear is considered to be the main wear pattern and an important tool life index in hard turning, and it has been intensively investigated by Huang and Liang [7]. On the other side, to improve the cutting edge strength, the cutting wedge angle of the CBN tool is generally greater than 90° with a large negative rake angle. The effective rake angle will become positive as crater wear progresses. This process results in a decrease of the cutting wedge angle. Since the CBN tool used in hard turning is brittle in nature, microchipping and/or tool breakage may occur as the possible results of the change of the wedge angle before tool flank wear reaches the pre-specified flank wear length criterion. In order to better predict tool life, it is important to model the progression of crater wear in addition to that of flank wear in hard turning. The objective of this study is to model the tool crater wear rate in hard turning by considering the effect of tool geometry, cutting condition, and material properties of the tool and the workpiece for the steady state wear growth process.

Numerous models have been proposed to describe the general wear volume loss and/or wear rate for different wear mechanisms, including some applications in metal cutting as discussed in [7]. In modelling tool wear in metal cutting, typically only one or two individual wear mechanisms were studied [8–11]. However, in the actual cutting tool, wear is often attributed to the combination of abrasion, adhesion, and diffusion. Furthermore, the effect of cutting condition, tool geometry, and/or material properties has not been explicitly investigated in most of the documented approaches. There is therefore a need to understand tool wear as a summation of the abrasion, adhesion, and diffusion effects as a function of cutting condition, tool geometry, and material properties. Besides the CBN tool flank wear study [7], a systematic approach to model the tool crater wear rate in hard turning is yet to be examined.

First, the crater geometry, chip velocity variation, and interface stress distribution are formulated as relevant to the geometry of tool crater. Then, the wear volume loss mechanisms due to abrasion, adhesion, and diffusion are discussed respectively. The crater wear rate is subsequently modelled based on the distributions of temperature, normal stress, and chip velocity on the tool-chip interface. Finally, the proposed model is experimentally verified in finish turning hardened of 52100 bearing steel under various cutting conditions.

2 Crater wear progression modelling in finish hard turning

2.1 Finish hard turning crater geometry

As shown in Fig. 1, the undeformed chip thickness is not uniform along the cutting edge in typical hard turning. The most

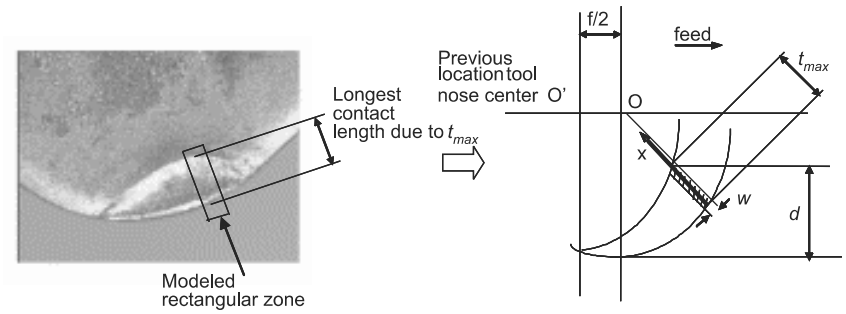

Fig. 1. Cutting geometric schematic for crater wear modelling

severe crater wear often takes place where the chip thickness has its maximum value $t_{\max}$ because the tool cutting edge of this location is expected to undergo the highest stress and temperature condition relative to other locations. Based on cutting geometry, $t_{\max}$ is defined as

$$t_{\max} = r - \sqrt{r^2 + f^2 - 2f\sqrt{2rd - d^2}}. \tag{1}$$

Therefore, the rectangular region with a width w and thickness of $t_{\max}$ shown in Fig. 1 (*left*) is of interest in this study. This rectangular zone corresponds to the tool-chip interface along the X axis as shown in Fig. 2.

Since cutting force without flank wear and cutting temperature do not show appreciable change unless crater wear becomes excessive, it is common to assume that the chip formation process is unaffected by the development of crater wear [8, 12]. Chip velocity along the contact length is important to the understanding of crater wear rate. Except for the conditions of extremely low cutting speed, there is material dragging-back occurring along the tool-chip interface. Tay et al. [13] assumed that velocity of the material at the tool rake face started at $\frac{V_{\text{chip}}}{3}$ at the tool edge and accelerated uniformly to V_{chip} within half the measured contact length. Considering the equal size of the sticking zone and the sliding zone [13, 14], the material along the tool-chip interface here is assumed to accelerate exponentially from zero velocity to V_{chip} within half the measured contact length as shown in Fig. 3.

Figure 3 also shows the distribution of normal stress. The transition of the uniform normal stress distribution from the tool tip to a power relationship is considered to take place at the mid-

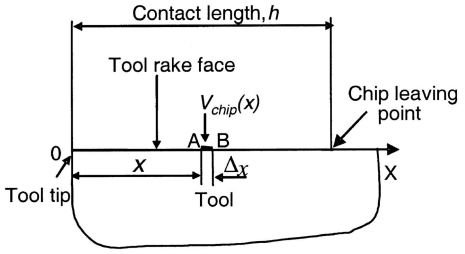

Fig. 2. Schematic of the tool-chip interface

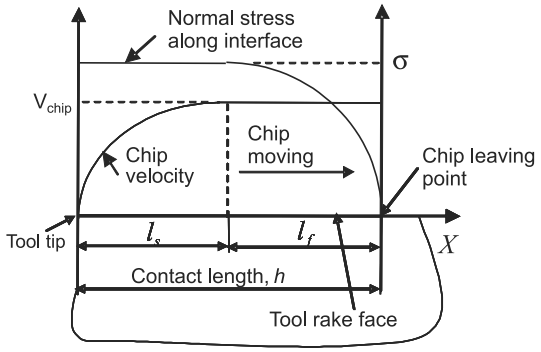

Fig. 3. Chip velocity and normal stress models along the tool-chip interface

point of contact length as [15] (b in [15] is taken as 0.5 here)

$$\sigma(x) = \frac{1.5N}{w(h + 0.5l_s)} \quad \text{for} \quad 0 \leqslant x < l_s$$

or

$$\frac{1.5N(h-x)^{0.5}}{w(h + 0.5l_s)(h-l_s)^{0.5}} \quad \text{for} \quad l_s < x \leqslant h. \tag{2}$$

2.2 Wear mechanisms along rake face in finish hard turning

2.2.1 Modelling of abrasive wear

Abrasive wear is the damage to a component surface due to the relative motion to that surface of either harder asperities or hard particles trapped at the interface. As discussed in [7], the dominant abrasive tool wear mechanism in CBN hard turning is the three-body wear with cementite and/or the CBN particle as the abrasive particles.

Considering an infinitesimal segment AB with length Δx in Fig. 2, which coincides with the X axis in Fig. 1, the total volume loss during the time interval Δt can be expressed as [7]:

$$\hat{V}_{\text{wear-abrasion}}(x) = K_{\text{abrasion}} K \left(\frac{P_a(x)^{n-1}}{P_t(x)^n} \right) V_{\text{chip}}(x) w \Delta x \sigma(x) \Delta t \tag{3}$$

where K_{abrasion} is the dimensionless abrasive wear coefficient depending on the given tool/workpiece combination; K and n is a known function of $\frac{P_t}{P_a}$, or Γ, as [11]:

$$\begin{aligned} &n = 1.0,\ K = 0.333, \quad \text{for} \quad \Gamma < 0.8; \\ &n = 3.5,\ K = 0.189, \quad \text{for} \quad 1.25 > \Gamma > 0.8; \\ &n = 7.0,\ K = 0.416, \quad \text{otherwise.} \end{aligned} \tag{4}$$

If more than one kind of abrasive particle exists along the interface, the total tool volume loss is attributed to different abrasive particles. Due to adhesive wear, some particles are generated as the result of the broken microwelds after tool passes the chip surface. Generally, the hardness of these particles is on the same order of that of bulk material, which is much lower than those of cementite and/or CBN particles. The tool volume loss due to these particles is neglected in this study.

The hardness of the abrasive particles (Fe_3C and/or CBN) [10, 16] and uncoated CBN tool [17] can be expressed as functions of temperature as (T is in °C):

$$\begin{aligned} &P_{\text{cementite}} = 11760e^{-16.3\times10^{-4}T}\,\text{N/mm}^2 \\ &P_{\text{CBN}} = 45000 - 4.324T\,\text{N/mm}^2 \quad (0\,^\circ\text{C} < T < 925\,^\circ\text{C}) \\ &P_{\text{tool-uncoated}} = 37500 - 24.7T\,\text{N/mm}^2 \quad (0\,^\circ\text{C} < T < 900\,^\circ\text{C}) \end{aligned} \tag{5}$$

2.2.2 Modelling of adhesive wear

The actual contact area along the tool/workpiece interface is made up of asperities, which may form microwelds under high

temperature and high stress. Due to the relative movement between the tool and the workpiece, shearing can take place either at the original interface or along a path below or above it, causing adhesive wear. Based on the approach in [7], the total volume loss due to adhesion is considered as contact length independent. The wear on the infinitesimal segment AB, in Fig. 2, is related to the length ratio of Δx over the whole contact length as follows:

$$\hat{V}_{\text{wear-adhesion}}(x) = \frac{\Delta x}{h} K_{\text{adhesion}} e^{aT(x)} V_{\text{chip}}(x) w \sigma(x) \Delta t \tag{6}$$

where K_{adhesion} is the adhesive wear coefficient with a unit of m^3/N. It is treated as a constant related to tool/workpiece combination.

2.2.3 Modelling of diffusive wear

A CBN particle itself is chemically stable with the steel workpiece even under high temperature and high stress, but the binder materials used in the CBN tool are relatively unstable under typical cutting conditions. The diffusion of binder material causes tool volume loss in hard turning, and results in the release of CBN particles. The concentration gradient over the tool-chip interface can be expressed as [9]:

$$\left.\frac{\partial c}{\partial y}\right|_{y=0} = -C_0 \sqrt{\frac{V_{\text{chip}}(x)}{\pi D(x) x}}. \tag{7}$$

Assuming that chip velocity $V_{\text{chip}}(x)$ and the coefficient of diffusion $D(x)$ are unchanged over the segment AB, the average concentration gradient over AB is

$$\begin{aligned}\frac{\mathrm{d}c}{\mathrm{d}y_{\text{ave}}}(x) &= -\frac{1}{\Delta x} C_0 \sqrt{\frac{V_{\text{chip}}(x)}{\pi D(x)}} \int_x^{x+\Delta x} x^{-\frac{1}{2}}\,\mathrm{d}x \\ &= -\frac{2C_0}{\Delta x} \sqrt{\frac{V_{\text{chip}}(x)}{\pi D(x)}} (\sqrt{x+\Delta x} - \sqrt{x}).\end{aligned} \tag{8}$$

Based on Fick's first law, the average flux rate along the interface is

$$\begin{aligned}J_{\text{ave}} &= -D \frac{\mathrm{d}c}{\mathrm{d}y_{\text{ave}}}(x) \\ &= -\frac{2C_0}{\Delta x} \sqrt{\frac{V_{\text{chip}}(x)}{\pi D(x)}} (\sqrt{x+\Delta x} - \sqrt{x}) \ \text{atoms}/\text{m}^2\text{s}.\end{aligned} \tag{9}$$

The coefficient of diffusion D is a function of temperature as [9, 18]

$$D(x) = D_0 e^{-\frac{Q}{R(T(x)+273)}}. \tag{10}$$

The diffusive wear loss over AB during Δt is defined by the material property, the average flux rate J_{ave}, the contact time, and the total new sliding surface [7]. Given the expression of J_{ave} as Eq. 9, the diffusive wear loss can be expressed as discussed in [7]:

$$\hat{V}_{\text{wear-diff}}(x) = K_{\text{diff}} e^{-\frac{K_Q}{T(x)+273}} \sqrt{V_{\text{chip}}(x)} (\sqrt{x+\Delta x} - \sqrt{x}) w \Delta t \tag{11}$$

where K_{diff} is the diffusive wear coefficient, with a unit of $\text{ms}^{-\frac{1}{2}}$, governed by the tool-workpiece combination.

2.3 Tool crater wear rate model

Considering the segment AB with width of cut w as shown in Fig. 2, the increase of tool crater during Δt is $\Delta K_T(x)$. The volume of tool material lost $\Delta V_{\text{wear}}(x)$ along AB can be approximated by

$$\Delta V_{\text{wear}}(x) = w \Delta x \Delta K_T(x). \tag{12}$$

The volume loss over the segment AB along the tool rake face is due to the combined effects of abrasion, adhesion, and diffusion during Δt, that is,

$$\Delta V_{\text{wear}}(x) = \hat{V}_{\text{wear-abrasion}}(x) + \hat{V}_{\text{wear-adhesion}}(x) + \hat{V}_{\text{wear-diff}}(x). \tag{13}$$

Based on Eqs. 3, 6, 11, and taking the time limit, the crater wear rate at over AB can be expressed as

$$\begin{aligned}\frac{\mathrm{d}K_T(x)}{\mathrm{d}t} =& K_{\text{abrasion}} K \left(\frac{P_a(x)^{n-1}}{P_t(x)^n}\right) V_{\text{chip}}(x) \sigma(x) \\ &+ \frac{1}{h} K_{\text{adhesion}} e^{aT(x)} V_{\text{chip}}(x) \sigma(x) \\ &+ K_{\text{diff}} e^{-\frac{K_Q}{T(x)+273}} \sqrt{V_{\text{chip}}(x)} \frac{(\sqrt{x+\Delta x} - \sqrt{x})}{\Delta x}.\end{aligned} \tag{14}$$

The five constants of wear rate model K_{abrasion}, K_{adhesion}, a, K_{diff}, and K_Q, are to be calibrated based on experimental data for the specific tool and workpiece combination involved.

3 Experimental validation

3.1 The general approach of modelling crater wear progression

Given tool geometry and cutting conditions, namely, cutting speed, depth of cut, and feedrate, $t_{\max}$ can be calculated using Eq. 1. With the information of material properties of the workpiece and the CBN tool in turning hardened steel, the process information, such as cutting forces, shear angle, shear flow stress, and the interface temperature distribution can be estimated by applying modified predictive machining theory [19] for a fresh tool.

With known and/or calibrated wear coefficients, the tool crater wear rate can be estimated. Based on the estimated wear rate, the new wear profile after a time interval can be predicted. The iteration will go on until microchipping or breakage happens and/or it reaches the tool flank wear criterion. Figure 4 depicts this modelling approach.

3.2 Model validation

Hardened AISI 52100 bearing steels with hardness 62 Rockwell were used as the workpiece for experimental validation. In order to simulate the practical hard turning process, bar dry facing is performed on a horizontal lathe (Hardinge T-42SP) using

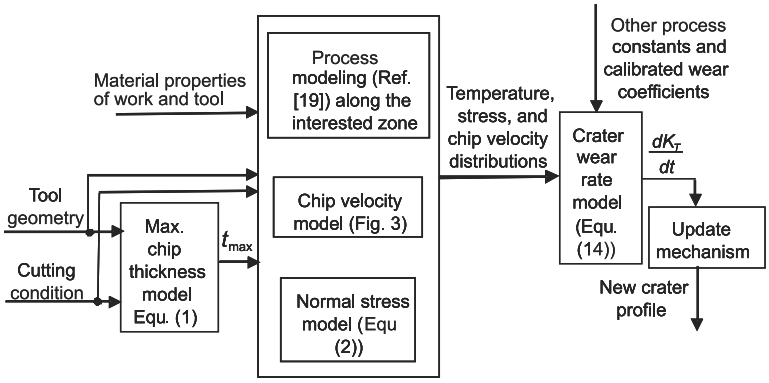

Fig. 4. The general approach to model crater wear progression in hard turning

a low CBN content tool insert (Kennametal KD050). The geometry of KD050 is specified by Kennametal CNGA-432S0420 (ISO CNGA120408S01020), with a $-20°$ and 0.1 mm wide edge chamfer and a 0.8 mm nose radius. The used tool holder is a Kennametal DCLNR-164D (ISO DCLNR-164D). The cutting is stopped when sudden force jump signaling a tool chipping. The size of crater wear generated was measured using an optical microscope (Zygo NewView 200).

Turning 52100 steel (62 HRc) using Kennametal KD050 CBN insert, the work in [7] examined tool flank wear progression under three cutting conditions (speed = 1.52 m/s, feed = 0.076 mm/rev, depth of cut = 0.203 mm; speed = 2.29 m/s, feed = 0.168 mm/rev, depth of cut = 0.203 mm; and speed = 1.52 m/s, feed = 0.076 mm/rev, depth of cut = 0.102 mm). Since the same tool/workpiece combination is used in this study, the coefficients in Eq. 14 can be calibrated based on the wear data in [7] to result in a crater wear rate model as:

$$\frac{\mathrm{d}K_T(x)}{\mathrm{d}t} = 0.0295K\left(\frac{P_a(x)^{n-1}}{P_t(x)^n}\right)V_{\mathrm{chip}}(x)\sigma(x) + 1.4761\times10^{-14}e^{9.0313\times10^{-4}T}\frac{1}{h}V_{\mathrm{chip}}(x)\sigma(x) + 5.7204\times10^{6}e^{-\frac{20460}{T+273}}\sqrt{V_{\mathrm{chip}}(x)}\frac{(\sqrt{x+\Delta x}-\sqrt{x})}{\Delta x}. \quad (15)$$

The force model and the crater wear model presented herein are applicable only if the chip formation process happens within the tool chamfer zone. Three sets of scenarios have been chosen to validate the proposed model while satisfying the tool chamfer zone requirement. They are: (1) cutting speed is 1.52 m/s, feedrate is 0.076 mm/rev and depth of cut is 0.102 mm; (2) cutting speed is 1.52 m/s, feedrate is 0.076 mm/rev and depth of cut is 0.152 mm; and (3) cutting speed is 2.29 m/s, feedrate is 0.061 mm/rev and depth of cut is 0.203 mm. In these cases, the contact length is observed to be limited to within the chamfer zone.

The typical predicted distributions of chip velocity, normal stress, temperature, and the wear rate in scenario (1) are shown in Fig. 5. It can be seen that the crater wear rate is not uniform

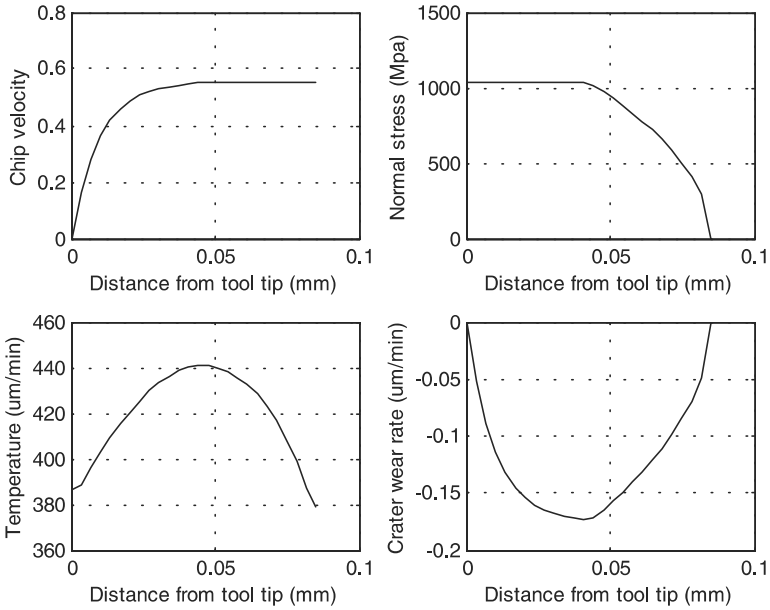

Fig. 5. Chip velocity, normal stress, temperature, and wear rate distributions under scenario (1)

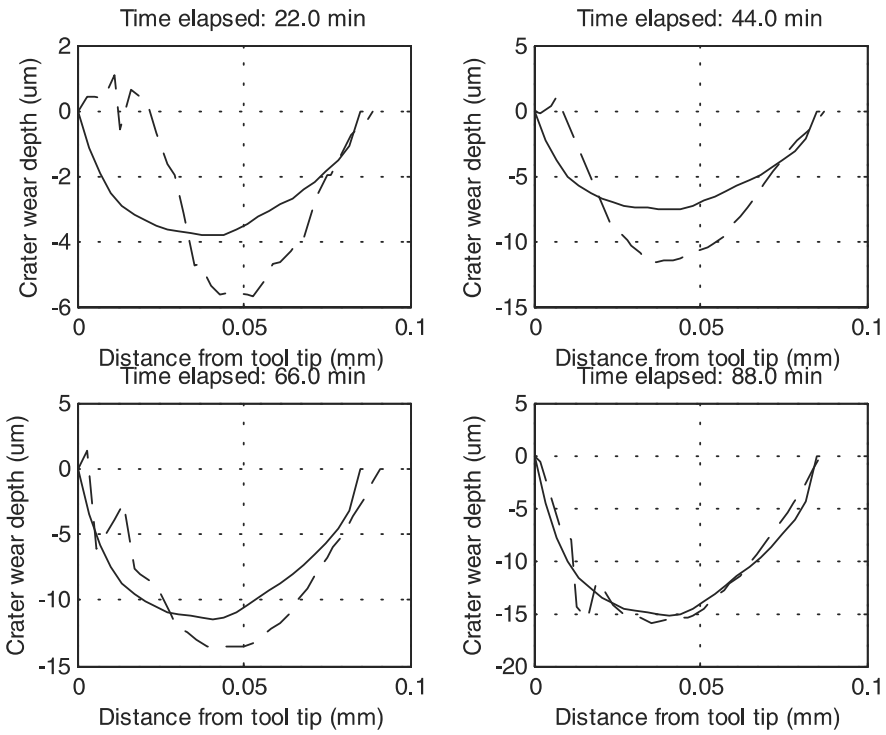

Fig. 6. Comparisons of prediction (*solid* line) to measurement (*dashed* line) under scenario (1)

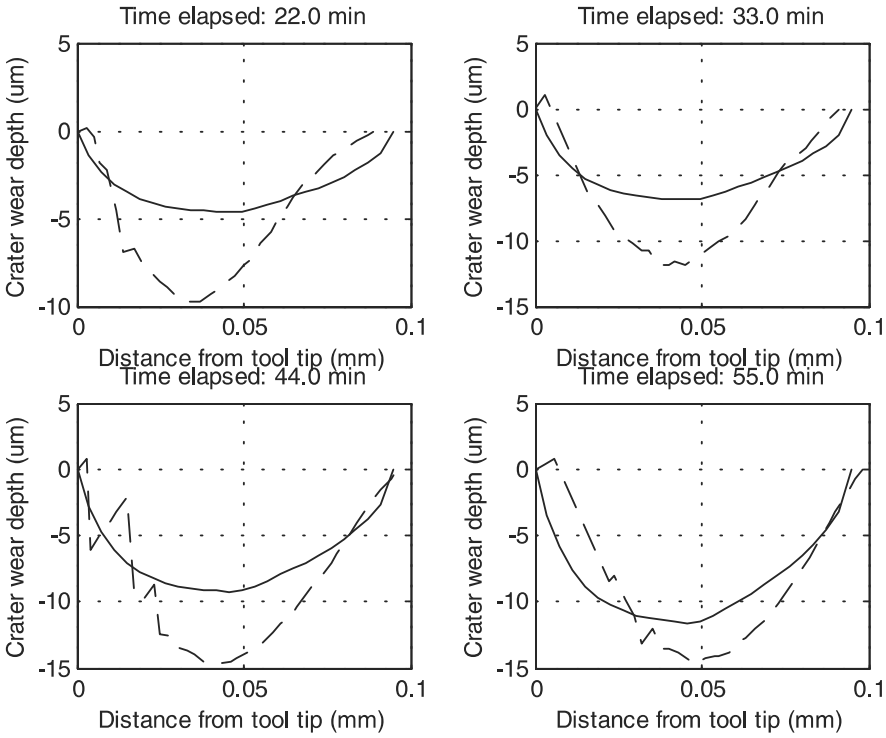

Fig. 7. Comparisons of prediction (*solid* line) to measurement (*dashed* line) under scenario (2)

and it reaches its maximum value around the midpoint of the tool/chip contact length. This predicted crater wear distribution matches that of general observations. The comparisons between the crater wear profile prediction and experimental measurement are shown in Figs. 6–8. Due to short tool life under scenario (3), only two measurements were recorded. Noticeable deviations are observed during the break-in wear period. It is considered reasonable because the initial wear loss during the break-in wear is stochastic and beyond the modelling realms of the presented approach, which targets the steady-state wear progression. Since

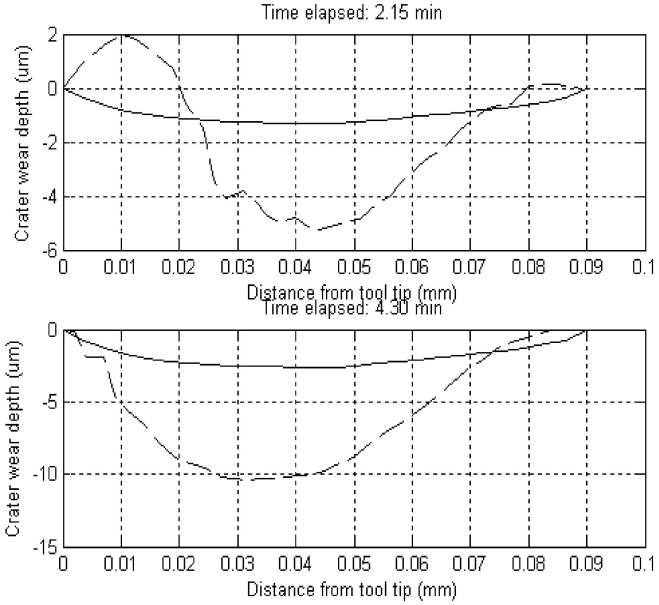

Fig. 8. Comparisons of prediction (*solid* line) to measurement (*dashed* line) under scenario (3)

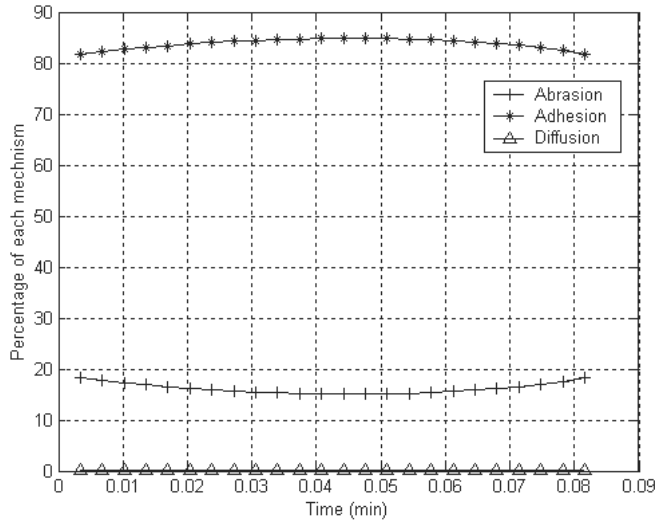

Fig. 9. Contribution percentage of different wear mechanisms under scenario (1)

the CBN tool is brittle and easy to microchip under the aggressive cutting conditions, especially with high cutting speed, such as in scenario (3), the model predictions tend to underestimate the wear depth profile as shown in Fig. 8. Overall, the proposed approach predicts crater wear under scenarios (1) and (2) to an error within 15% in terms of the total steady state volume loss in the 88 min plot in Fig. 6 and the 55 min plot in Fig. 7 respectively.

Figure 9 shows the relative contribution of different wear mechanisms in the investigated scenarios based on model prediction. Adhesion mechanism contributes the most (above 80%), followed by abrasion, then diffusion. The fact that basically adhesion is the dominant wear mechanism in typical hard turning cases has also been drawn based on other observations [20].

4 Conclusion

In this paper, the general approach in modelling the CBN tool crater wear rate is formulated and validated over a wide range of cutting conditions. The main wear mechanisms in hard turning are summarised as abrasion, adhesion, and diffusion. Based on the modelling of cutting geometry, chip velocity, temperature distribution, and stress distribution, the wear volume losses due to abrasion, adhesion, and diffusion are specified respectively to model the total rate of crater wear. With this model, tool geometry, cutting condition, and tool/workpiece material properties are the only information required to predict the progression of tool crater wear. The proposed model is experimentally verified in turning hardened 52100 bearing steel using the KD050 low CBN content insert. The comparison between predictions and experimental data shows that the proposed model agrees with the crater wear progression observation to an error within 15% in terms of the total tool volume loss under the stable wear growth condition. Adhesion is found to be the main wear mechanism over the range of investigated cutting conditions.

The proposed predictive model can help improve cutting condition optimisation and tool geometry design in hard turning. The proposed approach primarily deals with the continuous hard turning process under practical cutting conditions. For interrupted hard cutting using CBN tools, the tool hardness and fracture toughness may play an important role in the wear progression [21]. To model the tool crater wear rate in interrupted hard cutting in general, the tool hardness and fracture toughness may need to be further addressed.

Acknowledgement The authors wish to express their gratitude to Mr. Ty G. Dawson at Georgia Tech for discussions and his assistance during the machining experimentation.

References

1. Konig W, Hochschule T, Komanduri R, Schenectady D, Tonshoff HK (1984) Machining of hard materials. Ann CIRP 33(2):417–427.
2. Konig W, Berktold A, Koch KF (1993) Turning vs. grinding. Ann CIRP 42(1):39–43
3. Tönshoff HK, Arendt C, Ben Amor R (2000) Cutting of hardened steel. Ann CIRP 49(2):547–566
4. Turley DM (1974) A scanning electron microscopy study of attrition wear in tungsten carbide pin reamers. Wear 77:259–266
5. Moore DF (1975) Principles and application of tribology. Pergamon, Oxford
6. Chou Y, Barash MM, Review on hard turning and CBN cutting tools. SME Technical Paper MR95-214, pp 1–12
7. Huang Y, Liang SY (2004) Modeling of CBN tool flank wear progression in finish hard turning. ASME J Manuf Sci Eng 126(1):98–106
8. Usui E, Shirakashi T, Kitagawa T (1978) Analytical prediction of three dimensional cutting process, part 3: cutting temperature and crater wear of carbide tool. J Eng Ind 100:236–243
9. Kannatey-Asibu E Jr (1985) A transport-diffusion equation in metal cutting and its application to analysis of the rate of flank wear. J Eng Ind 107:81–89

10. Kramer BM Judd PK (1985) Computational design of wear coating. J Vac Sci Technol A3(6):2439–2444
11. Kramer BM (1986) Predicted wear resistances of binary carbide coatings. J Vac Sci Technol A4(6):2870–2873
12. Trigger KJ, Chao BT (1956) The mechanisms of crater wear of cemented carbide tools. Trans ASME 78:1119–1126
13. Tay AO, Stevenson MG, de Vahl DG (1974) Using the finite element method to determine temperature distributions in orthogonal machining. Proc Inst Mech Eng 188:627–638
14. Zorev NN (1966) Metal cutting mechanics. Pergamon, Oxford
15. Li X (1997) Development of a predictive model for stress distributions at the tool-chip interface in machining. J Mater Process Technol 63:169–174
16. Tlusty J (2000) Manufacturing processes and equipment. Prentice-Hall, Upper Saddle River, NJ
17. Childs THC, Maekawa K, Obikawa T, Yamane Y (2000) Metal machining: theory and applications. Wiley, New York
18. Armarego EJA, Brown RH (1969) The machining of metals. Prentice-Hall, Englewood Cliffs, NJ
19. Huang Y, Liang SY (2003) Cutting forces modeling considering the effect of tool thermal property-application to CBN hard turning. Int J Mach Tools Manuf 43(3):307–315
20. Chou Y (1994) Wear mechanism of cubic boron nitride tools in precision turning of hardened steels. Dissertation, Purdue University, IN
21. Chou YK, Evans CJ (1999) Cubic boron nitride tool wear in interrupted hard cutting. Wear 225–229:234–245